BIOCHEMISTRY
including biophysical chemistry & molecular biology
Article

Biochemistry **2009,** *48,* 8413–8421 8413
DOI: 10.1021/bi9010607

Structural Dynamics of Soluble Chloride Intracellular Channel Protein CLIC1 Examined by Amide Hydrogen−Deuterium Exchange Mass Spectrometry†

Stoyan H. Stoychev,‡ Christos Nathaniel,‡ Sylvia Fanucchi,‡ Melissa Brock,§ Sheng Li,§ Kyle Asmus,§ Virgil L. Woods Jr.,*,§ and Heini W. Dirr*,‡

‡*Protein Structure−Function Research Unit, School of Molecular and Cell Biology, University of the Witwatersrand, Johannesburg 250, South Africa, and* §*Department of Medicine and Biomedical Sciences Graduate Program, University of California, San Diego, 9500 Gilman Drive, La Jolla, California 92093*

Received June 23, 2009

ABSTRACT: Chloride intracellular channel protein 1 (CLIC1) functions as an anion channel in plasma and nuclear membranes when its soluble monomeric form converts to an integral-membrane form. The transmembrane region of CLIC1 is located in its thioredoxin-like domain 1, but the mechanism whereby the protein converts to its membrane conformation has yet to be determined. Since channel formation in membranes is enhanced at low pH (5 to 5.5), a condition that is found at the surface of membranes, the structural dynamics of soluble CLIC1 was studied at pH 7 and at pH 5.5 in the absence of membranes by amide hydrogen−deuterium exchange mass spectrometry (DXMS). Rapid hydrogen exchange data indicate that CLIC1 displays a similar core structure at these pH values. Domain 1 is less stable than the all-helical domain 2, and, while the structure of domain 1 remains intact, its conformational flexibility is further increased in an acidic environment (pH 5.5). In the absence of membrane, an acidic environment appears to prime the solution structure of CLIC1 by destabilizing domain 1 in order to lower the activation energy barrier for its conversion to the membrane-insertion conformation. The significantly enhanced H/D-exchange rates at pH 5.5 displayed by two segments (peptides 11−31 and 68−82) could be due to the protonation of acidic residues in salt bridges. One of these segments (peptide 11−31) includes part of the transmembrane region which, in the solution structure, consists of helix α1. This helix is intrinsically stable and is most likely retained in the membrane conformation. Strand β2, another element of the transmembrane region, displays a propensity to form a helical structure and has putative N- and C-capping motifs, suggesting that it too most likely forms a helix in a lipid bilayer.

Chloride intracellular channel (CLIC) proteins are expressed as soluble proteins without a leader sequence but have been shown to form anion channels in plasma and intracellular membranes (*1*). Although their physiological roles are uncertain, they have been implicated in a range of processes such as bone resorption (*2*), regulation of cell motility (*3*), apoptosis (*4*, *5*), tubulogenesis (*6*) and β-amyloid-induced neurotoxicity (*7*). The CLIC proteins are unusual for ion channels in that they exist in cells both as soluble and integral membrane forms (*8*−*10*). Although high-resolution crystal structures exist for soluble forms of CLICs (*11*−*17*), very little is known about the mechanism whereby they convert to their membrane-inserted forms. Further, the structures of these membrane-inserted forms, the stoichiometry required to form a channel and the mechanism of ion conductance are unknown. Soluble CLICs are structural homologues of the canonical cytosolic glutathione transferases (GSTs[1]), notably the class Omega GST (*11*). Unlike CLICs, GSTs are dimeric and do not insert into membranes. The monomeric CLIC structure is composed of two domains: a thioredoxin-like domain 1 and an all-helical domain 2 (for CLIC1, see Figure 1). The membrane-spanning region is located in the smaller thioredoxin-like domain, and there is substantial evidence demonstrating that the amino acid sequence corresponding to the amphipathic α1β2 motif forms the transmembrane region (*6*, *11*, *12*, *18*−*20*) (Figure 1). Domain 2 appears not to contribute toward either membrane insertion or channel functioning (*20*). During the conversion of the soluble precursor to an integral-membrane form, strand β1 and the α1β2 motif are expected to undergo conformational changes that will expose buried hydrophobic regions and allow the replacement of protein−protein interactions with protein−lipid interactions (*21*).

Triggers that initiate structural rearrangements in soluble-to-membrane proteins include factors such as redox effects, low pH, lipid charge and membrane composition, the binding of signaling molecules and proteolysis (*22*−*26*). Oxidation of CLIC1 in the presence of membranes has been shown to trigger

†This work was supported by the University of the Witwatersrand, the South African National Research Foundation (Grant 205359), the South African Research Chairs Initiative of the Department of Science and Technology and National Research Foundation (Grant 64788), and by grants from the Innovative Technologies for the Molecular Analysis of Cancer (IMAT) program (CA099835, and CA118595, V.L.W.), NIH Grants AI076961, AI081982, AI2008031, AI072106, AI068730, GM037684, GM020501, GM066170, (V.L.W.), and a Discovery Grant (UC10591) from the University of California IUCRP Program, BiogenIDEC corporate sponsor (V.L.W.).

*Corresponding authors. H.W.D.: tel, +27 11 7176352; fax, +27 11 7176351; e-mail, heinrich.dirr@wits.ac.za. V.L.W.: tel, (858) 534-2180; fax, (858) 534-2606; e-mail, vwoods@ucsd.edu.

[1]Abbreviations: CLIC1, chloride intracellular channel protein 1; DXMS, hydrogen−deuterium exchange mass spectrometry; GuHCl, guanidine hydrochloride; H/D, hydrogen/deuterium; GST, glutathione transferase; TMR, transmembrane region.

Published on Web 08/03/2009

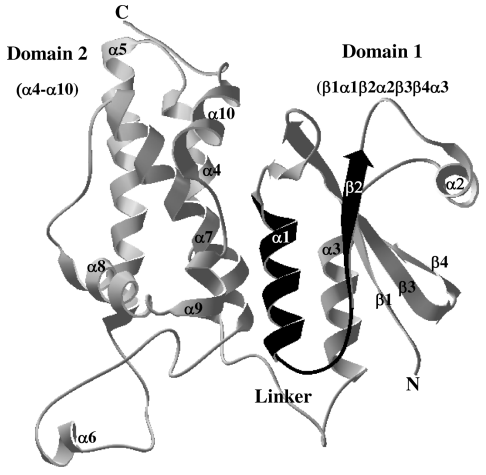

FIGURE 1: Ribbon representation of the crystal structure of soluble CLIC1 (PDB code 1k0m (*11*)). Domain 1 consists of helices α1, α2 and α3 and strands β1, β2, β3 and β4. Domain 2 consists of helices α4 to α10. The linker region between the domains is indicated. The secondary structural elements α1 and β2, that constitute the transmembrane region, are colored in black.

a soluble-to-membrane partitioning of the protein (*27*). CLIC channel formation and activity have been demonstrated to be highly pH-dependent (*10*, *20*, *28*), in that a low pH (5 to 5.5) significantly enhances the rate of CLIC1 insertion into membranes (*28*). An acidic pH environment at the surface of membranes results from the attraction of protons by the negatively charged polar head groups in the lipid bilayer (*29*−*31*).

Water-soluble proteins that insert into membranes follow multistep processes that include pH-dependent structural changes that enable them to partition into lipid bilayers (*32*). Many bacterial pore-forming toxins, for example, have been reported to form acid-induced molten globule-like intermediates for membrane insertion (*23*, *31*, *33*−*35*). Since the molecular mechanism of how the structure of soluble CLIC1 is primed or altered for membrane insertion when it encounters the acidic environment near/at the surface of membranes is unknown, the conformational dynamics of soluble human CLIC1 was investigated as a function of pH (5.5−7.0) in the absence of membranes by amide hydrogen−deuterium exchange mass spectrometry (DXMS) (*36*−*39*). Hydrogen−deuterium exchange experiments provide information on the local stability of proteins, and we have identified and mapped the sequences most susceptible to pH-induced conformational changes at the level of the crystal structure of soluble CLIC1 (*11*) when the protein molecule moves from a neutral pH (cytosol) to an acidic pH of 5.5 (near/at membrane surface).

EXPERIMENTAL PROCEDURES

Expression and purification of recombinant CLIC1. Human CLIC1 was expressed as a fusion protein with SjGST from the pGEX-4T-1 plasmid (a gift from Samuel Breit, St. Vincent's Hospital and University of New South Wales, Australia) in *Escherichia coli* BL-21 cells and the CLIC1 purified as described previously (*11*, *40*). Purified CLIC1 was stored in 50 mM sodium phosphate buffer, pH 7, containing 1 mM DTT and 0.02% sodium azide. A molar extinction coefficient of 17170 M^{-1} cm^{-1} at 280 nm was used to quantify CLIC1.

Spectroscopic Measurements. Protein was 5 μM for fluorescence and far-UV CD and 40 μM for near-UV CD measurements in 50 mM sodium phosphate, 1 mM DTT and 0.02% sodium azide at pH 7.0 or pH 5.5. All measurements were made at 4 and 20 °C. Fluorescence measurements were conducted using a Jasco FP-6300 spectrofluorimeter with excitation at 280 nm and slit widths of 5 nm. Far- and near-UV CD measurements were carried out with a Jasco J-810 spectropolarimeter. Path length was 2 mm for far-UV CD and 5 mm for near-UV CD.

Hydrogen-Exchange Mass Spectrometry. (*a*) *Sample Preparation*. All samples, with the exception of the equilibrium-deuterated control, and buffers were prechilled on ice and prepared at 4 °C in the cold room. 15 μL of 0.50 mg/mL CLIC1 (pH 7.0) or 0.34 mg/mL CLIC1 (pH 5.5) in storage buffer (50 mM Na_2HPO_4, 1 mM DTT, 0.02% NaN_3 pH 7.0 or pH 5.5) was incubated with 45 μL of deuteration buffer (10 mM Na_2HPO_4, 150 mM NaCl in 99.9% D_2O, pH 7.0 or pH 5.5) for varying time periods. As the rate of amide H/D exchange is highly pH dependent, a decrease in pH by 1 unit reduces H/D exchange by approximately 10-fold (*41*). Since H/D exchange is expected to be about 30-fold slower at pH 5.5 than at pH 7.0, the on-exchange times for CLIC1 at pH 7.0 were 10, 30, 100, 300, 1000, and 3000 s, while the on-exchange times at pH 5.5 were 10, 30, 100, 300, 1000, 3000, 9000, 30000, and 90000 s. After the allocated time, the hydrogen−deuterium exchange reaction was stopped by adding 90 μL of quench buffer, pH 2.3 (0.8% formic acid, 17% glycerol, 0.8 M GuHCl for CLIC1 at pH 5.5 or 1.6 M GuHCl for CLIC1 at pH 7.0), and incubating the reaction mixture for 1 min with gentle mixing. In addition to the on-exchange samples, nondeuterated and equilibrium-deuterated controls were also prepared. For the nondeuterated control, 15 μL of CLIC1 (pH 7.0) or CLIC1 (pH 5.5) was incubated with a mixture of 45 μL of nondeuteration buffer (10 mM Na_2HPO_4, 150 mM NaCl, pH 7.0) and 90 μL of quench buffer. The equilibrium-deuterated control was prepared the night before the rest of the samples where 15 μL of CLIC1 (pH 7.0) or CLIC1 (pH 5.5) was incubated with 45 μL of equilibrium-deuterated buffer (0.8% formic acid in 99.9% D_2O) for 16−18 h at 25 °C. After the allocated time, the mixture of CLIC1 (pH 7.0) or CLIC1 (pH 5.5) and equilibrium-deuterated buffer was chilled to 0 °C and the exchange reaction was stopped through the addition of 90 μL of prechilled quench buffer. All samples, including the non- and equilibrium-deuterated controls, were aliquoted in triplicate, snap-frozen on dry ice (immediately after preparation) and express-mailed at dry ice temperature from the site of preparation (Johannesburg, South Africa) to San Diego, CA.

(*b*) *Sample Analysis*. Sample analysis was performed at the School of Medicine, University of California San Diego (UCSD), employing an apparatus that automatically thawed and proteolyzed frozen samples, followed by LC−MS analysis of the resulting peptides. Briefly, frozen protein samples were thawed and, at 0 °C, passed through a solid-phase pepsin column with 0.05% trifluoroacetic acid at 100 μL/min with 4 min exposure to pepsin. Again at 0 °C, the proteolytic products were passed through a C18 RP-HPLC column (Vydac 50 mm × 1 mm, 300 A) and eluted with a linear 4−36% acetonitrile gradient over thirty minutes. Initial peptide identification was done using collision induced dissociation (CID) on a Finigan LCQ electrospray ion trap mass spectrometer in data-dependent MS2 (tandem MS) mode with capillary temperature at 200 °C. All subsequent samples, including the nondeuterared and equilibrium-deuterated controls as well as 10−3000 s time points, were analyzed using the same mass spectrometer in profile mode.

(*c*) *Data Processing and Peptide Validation*. The sequence of each peptide was identified using the Sequest software

program (Thermo Finigan Inc.), which maps the raw spectral data to the sequence of CLIC1. The resulting peptide pool was quality checked using specialized software (Sierra Analytics, LLC, Modesto, CA) (*36*−*39*). Authenticity was validated by a good fit between the theoretical and experimental isotopic envelopes of each peptide. Additionally, parameters such as retention time, m/z range, centroid value and mapping score were scrutinized. The level of deuterium incorporation for each peptide was calculated by subtracting the centroid value of molecular isotope of partially deuterated peptide from the centroid value of nondeuterated peptide as per the method devised by Zhang and Smith (*42*). The procedure was automated through the use of the specialized software used to quality-check the peptide pool (*36*−*39*). Sublocalization of deuterium was performed next, where the partially deuterated peptides were mapped onto the primary sequence of CLIC1. The level of peptide overlap determines the resolution of this step, i.e., multiple overlapping fragmets can narrow the position of deuterium localization. In addition, overlapping fragments that differed by more than two deuterons were identified as outliers and deleted from further analysis.

Corrections for back-exhange, on average ~30%, were made by employing the methods used by Zhang and Smith (*42*):

$$D_O = (m - m_{0\%})/(m_{100\%} - m_{0\%}) \times N/0.75$$

where D_O is the average number of deuteriums per peptide at the time of the analysis, m is the average mass of the partially deuterated peptide, $m_{0\%}$ is the average mass of the nondeuterated peptide, $m_{100\%}$ is the average mass of the equilibrium-deuterated peptide and N is the number of peptide amide linkages in a peptide. Corrections for the final deuterium concentration, 75%, in each sample were also made. The number of peptide amide linkages in a peptide was calculated from

$$N = T_N - 2 - T_{Pro}$$

where $T_N - 2$ is the number of residues of the peptide minus the first two amino acids that cannot retain deuterium, and T_{Pro} is the number of proline residues found in the peptide. It must be noted that the back-exchange equation was shown to introduce an error in D_O. For three thousand peptides of random sequence and size this error was calculated to be at an averge of 5.5% with a standard deviation of 5.5% (*42*). Consequently, only differences of 10% or higher were deemed as significant when comparisons were drawn. Finally, matching peptides for pH 7 and pH 5.5 whose back-exchange values differed by more than 10% were discarded.

RESULTS

Global Structure of Soluble CLIC1. Fluorescence and CD spectroscopy were used to characterize the global structure of CLIC1 at low temperature (4 °C) and at 20 °C. The data shown in Figure 2 are consistent with the features of the crystal structure of CLIC1 (*11*, *43*) and indicate that the protein's conformation is not significantly affected by pH between 7 and 5.5 and by temperature between 4 and 20 °C. It is, therefore, unlikely that the labeling of CLIC1 with deuterium at low temperature involves an artifactual low temperature conformation of the protein.

CLIC1 Sequence and Pepsin Digestion. The CLIC1 sequence used in the H/D exchange study differs from that reported for the crystal structure, in that it has 2 additional

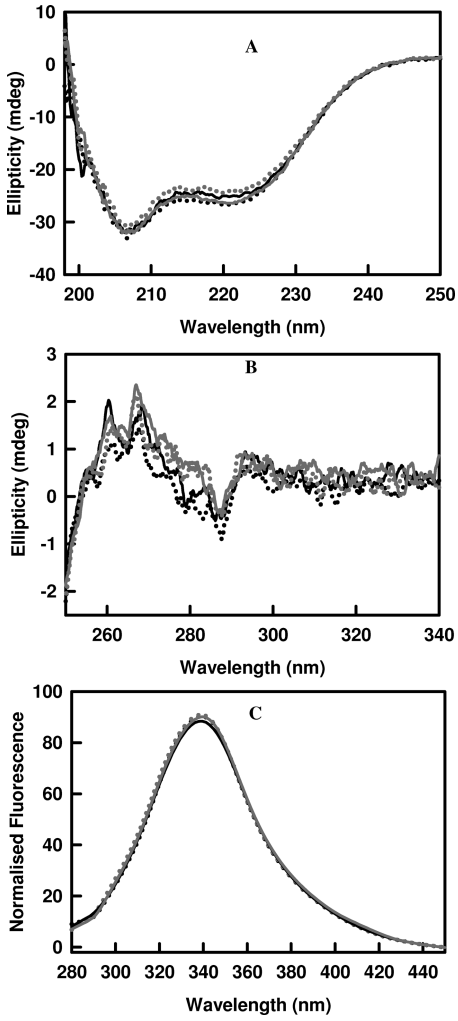

FIGURE 2: Far-UV CD spectra (A), near-UV CD spectra (B), and fluorescence emission spectra (C) for native CLIC1 at pH 7 (black) and pH 5.5 (gray). Spectra were recorded at 20 °C (solid line) and at 4 °C (dotted line). There are no significant changes in the secondary and tertiary structures of CLIC1 over this temperature range.

residues at the N-terminus due to the thrombin cleave site, and two mutations, E63Q and G151E (Figure 3). The numbering of all peptides reported in this study excludes the additional two residues at the N-terminus and corresponds to that for the structure. Pepsin digestion of CLIC1 in 1 M GuHCL and 0.8% (v/v) formic acid for a duration of 4 min over immobilized pepsin yields peptides that cover the entire sequence of CLIC1 at both pH 7 and pH 5.5. Of these peptides, 75 were well resolved and common to CLIC1 at pH 7 and pH 5.5 covering 95% of the sequence (Figure 3). The only region not covered is residues 42−54. The number of deuterons incorporated was measured for all 75 peptides, including peptides with multiple charge states, and of these, 21 peptides were chosen to generate the deuterium exchange data shown in the graphics. However, all 75 peptides were analyzed to ensure that the exchange data agreed with those of the 21 selected peptides. Of the 21 peptides, 7 come from the thioredoxin-like domain, domain 1, and 13 come from the all-helical domain 2 (Figure 3).

Hydrogen−*Deuterium Exchange at pH 7 and 5.5*. As the rate of amide H/D exchange is highly pH dependent and H/D exchange is expected to be about 30-fold slower at pH 5.5 than at pH 7.0 (*41*), the on-exchange time points for pH 5.5 are 30-fold longer (300, 3000, 9000, 30000, and 90000 s) than the

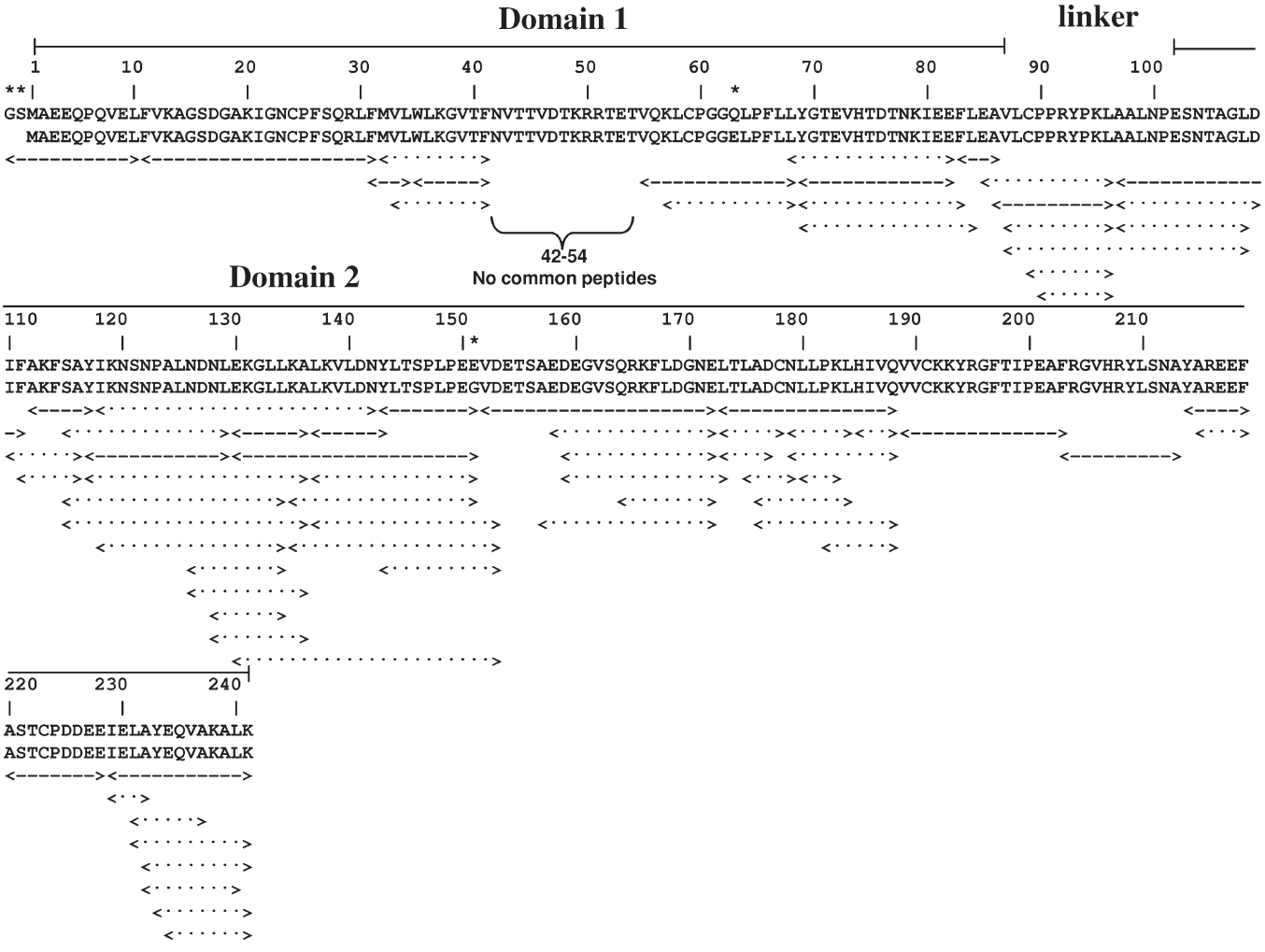

FIGURE 3: Sequence and peptic fragments of CLIC1. The sequence used in the DXMS study is shown above while that reported for the crystal structure of CLIC1 (PDB code 1k0m (*11*)) is shown below. Numbering is based on the structure's sequence. The asterisks indicate the differences between the sequences, as described under Results. The broken and dotted lines under the protein sequence indicate peptic fragments that are common to CLIC1 at pH 7 and pH 5.5. Peptides chosen for this study are shown by the broken lines. The only region not covered is residues 42−54. The regions corresponding to the two domains and the linker are indicated by the solid lines above the sequence.

corresponding time points for pH 7 (10, 100, 300, 1000, and 3000 s). Differences in deuteration of CLIC1-derived peptides at pH 5.5 and pH 7.0 and at the corresponding on-exchange time points were revealed by overlaying isotopic profiles of the individual peptides. For example, the changes in the isotopic profiles for peptides 11−31 and 68−82 indicate a more rapid shift toward a higher mass at pH 5.5 than at pH 7.0 (see Figure S1 in the Supporting Information).

The extents of deuteration at pH 7 for 10 s and at pH 5.5 for 300 s are similar and do not differ by more than 10% (Figure 4), indicating comparable core structures of the protein under these conditions. Further, the intensity of deuterium incorporation of soluble CLIC1 correlates well with structural parameters calculated for the crystal structure (PDB code 1k0m (*11*)), i.e., secondary structure, hydrogen bonding and solvent accessible surface area of the backbone (Figure 4), in agreement with the above spectroscopic data. The high levels of rapidly exchanging protons for the N-terminus comprising strand β1 and for peptide 152−172 comprising helix α6 are explained by their highly dynamic behavior in CLIC1, as indicated by a lack of well-defined electron density in some crystal structures (*11*).

Figure 5 shows deuterium incorporation profiles of the 21 chosen peptides at the five on-exchange times for each pH condition. No common peptides were obtained for the region covered by residues 42−54. To determine which peptides display significant changes in deuteration, we calculated the differences between pH 7 and pH 5.5 at the corresponding time points (Figure 6). Of the 21 peptides, 13 do not show significant differences in their levels of deuterium incorporation (i.e., differences are $< 10\%$) (Figure 6).

The 8 peptides that display exchange differences of $> 10\%$ (see Figure 6) are mapped onto the structure of CLIC1 together with their H/D exchange kinetics, as shown in Figure 7A. The data indicate that the protection of amide protons in much of domain 1 is affected by lowering the pH from 7 to 5.5 resulting in enhanced levels of H/D exchange in segments comprising portions of β1 (peptide 1−10), β1α1 (peptide 11−31), α2β3 (peptide 55−68) and β4α3 (peptide 68−82). Helix α1 forms part of the transmembrane region (TMR, residues 25−46 (*6*, *11*, *18*−*20*)) of membrane-inserted CLIC1 (Figure 1). The biggest increases in deuterium incorporation at pH 5.5 occur in peptides 11−31 and 68−82. Unfortunately, there were no common peptides for residues 42−46 (strand β2) which also form part of the TMR (Figure 1). However, nearly all amide protons in a peptide 42−48 obtained only at pH 5.5 are rapidly exchanged within 300 s, indicative of a highly flexible segment at least at this pH

(Figure 7A). Four segments in domain 2 also display enhanced levels of H/D exchange: the N- and C-terminal regions of α4 (peptides 97−111 and 117−129, respectively), the N- and C-terminal regions of α5 (peptides 117−129 and 143−151, respectively) and the C-terminal region of α7 and the loop connecting α7 to α8 (Figure 7A).

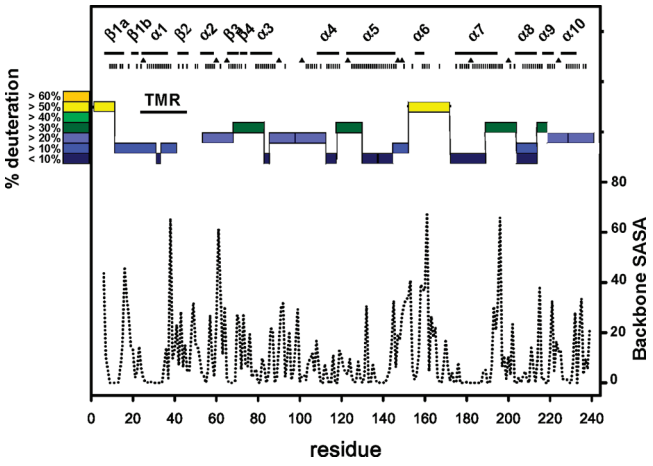

FIGURE 4: Exchange of amide protons of peptides from CLIC1 at pH 7 and at pH 5.5 for 10 and 300 s on-exchange times, respectively. The longer on-exchange time at pH 5.5 is to account for the 30-fold slower exchange rate at this pH (*41*). The percentages of deuterium incorporation are indicated by the color bar. The single color bars are for the levels of deuteration at both pH 7 and 5.5 except for segment 203−213, which has two color bars to show the difference in % deuteration at pH 7 (light blue) and pH 5.5 (dark blue). The solvent accessible surface area (SASA) of the backbone in CLIC1 (PDB code 1k0m (*11*)) was determined by GetArea (http://www.scsb.utmb.edu/getarea) and is shown by the broken line plot. The positions of α-helical (α) and *β*-strand (*β*) regions are shown by solid horizontal bars, prolines are indicated by diamonds, and backbone hydrogen atoms involved in hydrogen bonding interactions are labeled with vertical lines. TMR indicates the sequence (residues 25−46) that corresponds to the transmembrane region.

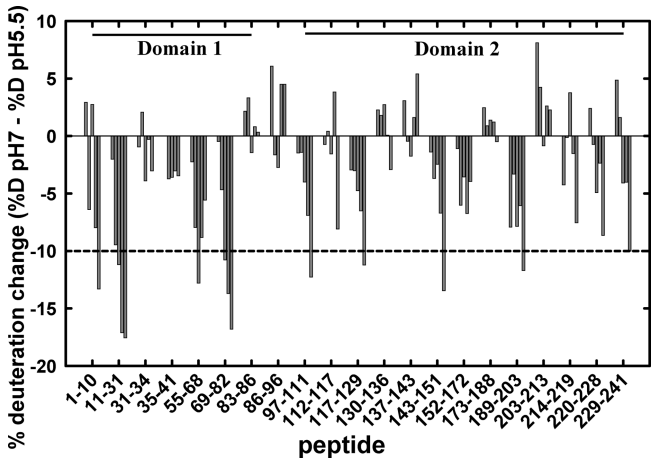

FIGURE 6: Differences in the level of deuteration of CLIC1 peptides upon lowering the on-exchange pH from 7 to 5.5. The % deuteration change (% D pH 7 to % D pH 5.5) for each peptide (sequence indicated on the *x*-axis) was calculated by subtracting the % of deuteration at pH 5.5 (% D pH 5.5) from the % of deuteration at pH 7 (% D pH7). Positive differences represent decreased levels of deuteration at pH 5.5, while negative differences represent increased deuteration at pH 5.5. Each peptide (sequence indicated on the *x*-axis) is represented by the difference calculated between pH 7 and pH 5.5 for the five on-exchange time points (vertical bars). The time points for pH 7 were 10, 100, 300, 1000, and 3000 s, whereas, given the 30-fold slower exchange rate at pH 5.5 (*41*), the corresponding time points at pH 5.5 were 300, 3000, 9000, 30000, and 90000 s. Differences of greater than 10% (broken line) are considered to be significant (see Experimental Procedures for further explanation). No data were obtained for residues 42−54 due to the absence of common peptides in this region. The peptides corresponding to the two domains are indicated by the two solid horizontal lines.

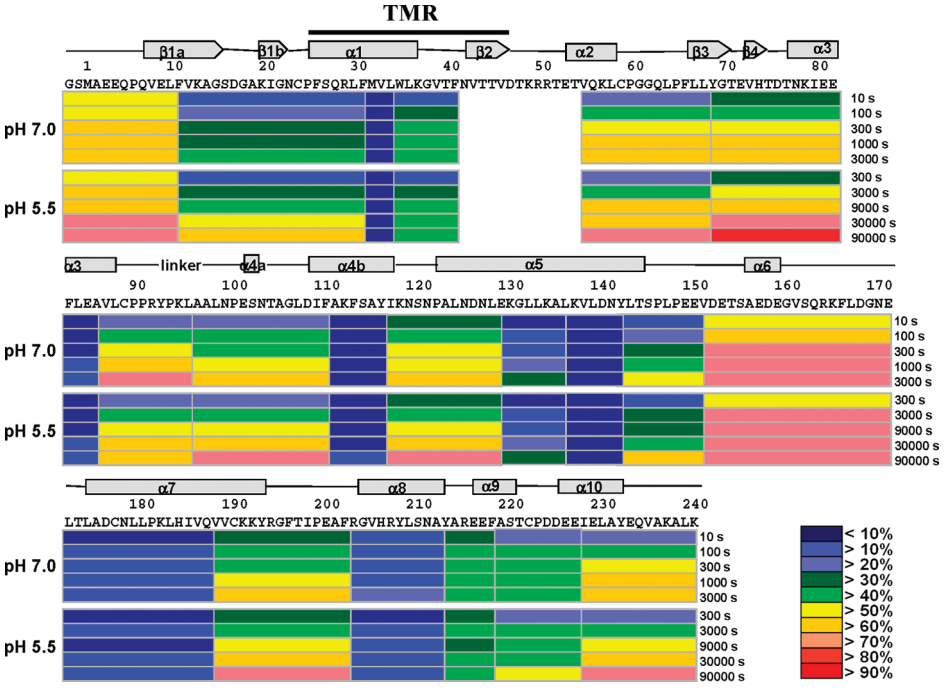

FIGURE 5: Amide hydrogen−deuterium exchange analysis of the effect of pH on CLIC1. Each pH condition (7.0 and 5.5) is divided into rows of blocks (peptides) that, from top to bottom, correspond to five on-exchange time points from 10 to 3000 s for pH 7, and from 300 to 90000 s for pH 5.5, as indicated. The longer on-exchange times at pH 5.5 are to account for the 30-fold slower exchange rate at this pH (*41*). The deuteration levels for each block (peptide) at each time point are shown by different colors as indicated by the color bar. The CLIC1 sequence and the α-helical (α) and *β*-strand (*β*) regions are shown above. TMR indicates the sequence (residues 25−46) that corresponds to the transmembrane region.

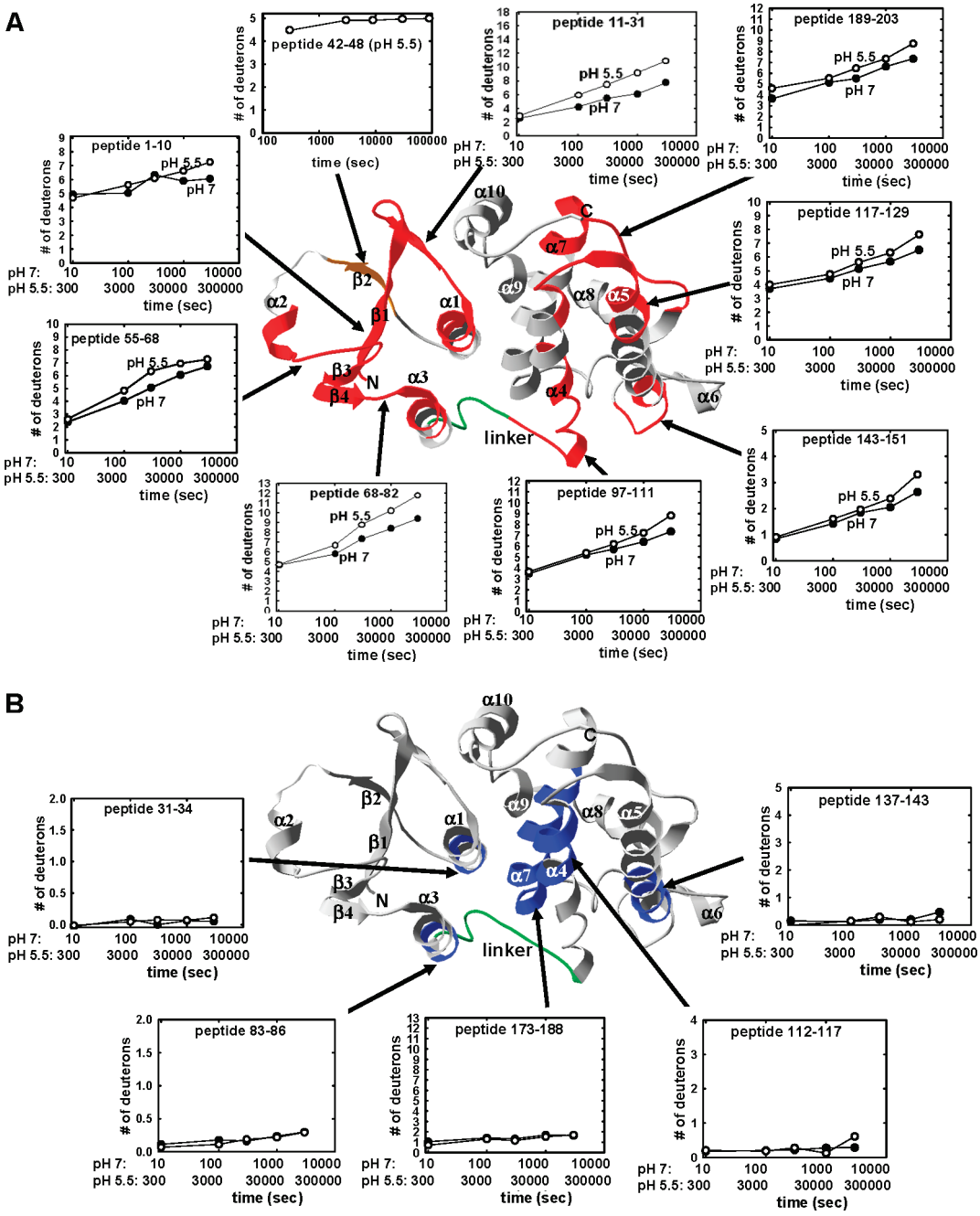

FIGURE 7: H/D exchange kinetics for CLIC1 segments mapped on the crystal structure of CLIC1 (PDB code 1k0m (*11*)). (A) The red ribbons represent the eight regions for which the difference in deuteration at pH 7 and pH 5.5 at least at one time point was > 10% (see Figure 6), while the orange ribbon represents the exchange data for a peptide (residues 42−48), in the transmembrane region, that was only obtained at pH 5.5. (B) The blue ribbons represent the five regions that display little or no deuterium incorporation at pH 7 and pH 5.5 (see Figure 5). α-Helices, *β*-strands, and the N- and C-termini are labeled. The linker region connecting the two domains is in green. The time axes for the H/D exchange kinetics at pH 7 and at pH 5.5 are shown and account for the 30-fold slower exchange rate at pH 5.5 (*41*). H/D exchange kinetics at pH 7 are in filled circles, and the kinetics at pH 5.5 are in open circles.

Figure 7B shows the peptides mapped on the structure of CLIC1 that display very little H/D exchange at pH 7 and 5.5 throughout the experiment. They include the C-terminal regions of α1 and α3 (peptides 31−34 and 83−86, respectively), both in domain 1, and the central-to-C-terminal region of α4 (peptide 112−117), the central-to-C-terminal region of α5 (peptide 137−143) and most of α7 (peptide 173−188), in domain 2. The stable and highly protected segments 31−34, 112−117 and 173−188 in CLIC1 correspond to regions in the structurally related rGST M1−1 that display no increase in amide H/D exchange (*44*). The H/D exchange kinetics data for several peptides from CLIC1 are shown in Figure S2 in the Supporting Information.

Overall, the amide H/D exchange results for soluble CLIC1 show that the all-helical domain 2 is more stable and better protected than the thioredoxin-like domain 1 when the pH is lowered from 7 to 5.5. The proximity of the stable segments 112−117, 137−143 and 173−188 in a bundle formed by helices 4, 5, and 7 (Figure 7B) indicates an important structural motif for the stability of the core of domain 2. The stability of helix 7 (equivalent to helix 6 in GSTs) is consistent with its putative role in the nucleation of GST folding (*45*).

DISCUSSION

Low pH conditions facilitate the appearance and activity of CLIC1 anion channels in membranes, although the mechanism involved remains to be determined (*10*, *20*, *28*). An acidic pH at the surface of a membrane (*29*, *31*) can function to prime or alter the structure of a soluble protein to achieve a lower activation energy barrier for its conversion to a membrane-insertion conformation (*31*, *46*). In contrast to other membrane-insertable proteins (*23*, *31*, *47*−*51*), CLIC1 does not undergo significant acid-induced structural changes in the absence of membranes (this study and ref (*43*)). Recently, it has been shown that the changes needed for the soluble antiapoptotic protein Bcl-x_L to convert to its membrane conformation also require both acidic conditions (pH 4.9) and the presence of membranes (*52*).

The H/D exchange data reported in this study indicate that the thioredoxin-like domain 1 of CLIC1 is less stable than domain 2, and that, while the structure of domain 1 remains intact, its stability is further reduced in an acidic environment (pH 5.5), a condition shown by others to facilitate the protein's insertion into membranes (*28*). The conformational stability of soluble CLIC1 has been shown to diminish substantially at pH 5.5, resulting in the formation of a partially unfolded intermediate not observed at pH 7 (*43*). Unfolding of the native protein to the nonmolten globule-like intermediate involves helix α1 the structural element in domain 1 that makes the majority of contacts with domain 2. Substantial evidence exists indicating that the amino acid sequence corresponding to the amphipathic α1β2 motif in domain 1 forms the transmembrane region that spans membranes (*6*, *11*, *18*−*20*). For this motif to function as a transmembrane region, it will have to become detached from domain 2 and then extend and refold into its membrane-insertable conformation. It is, therefore, possible that, as soluble CLIC1 encounters an acidic environment (e.g., pH 5.5) near the surface of a membrane, the enhanced flexibility and diminished stability of domain 1 allows it to loosen up and become primed for the structural changes needed for it to insert into membranes. While the conformation of the membrane-inserted transmembrane region is unknown, it is most likely to be helical. Helix α1 in soluble CLIC1 has a highly stable central region, as indicated by the absence of H/D exchange in peptide 31−34 at pH 7 and 5.5 (Figure 7B). When compared to most members of both the thioredoxin and GST superfamilies, the sequences of helix 1 in CLIC proteins display the highest propensities to form a helix according to the AGADIR helix−coil algorithm (*53*). Furthermore, helix 1 has an N-capping motif (Ser27) and a C-capping motif (Lys37), both of which can stabilize helical structures substantially (*54*). GST Kappa, a noncanonical GST, and calsequestrin, a member of the thioredoxin family, both of which are known to interact with membranes (*55*, *56*), also display high helix propensities for their corresponding helix 1 sequences. However, the sequence for helix 1 in class Omega GST, the closest structural homologue of CLIC1 (*11*), does not display as high a helical propensity. Since membrane spanning structures are typically helical, it is reasonable to assume that helix 1 is retained in membrane-inserted CLIC1. Although residues 42−46 in the transmembrane region form strand β2 in the crystal structure, this highly dynamic segment at pH 5.5 (Figure 7A) also exhibits a propensity to form a helix with potential N- and C-capping motifs.

Since membrane insertion of CLIC1 is favored at low pH (5−5.5), the involvement of protonation and electrostatic effects in bringing about structural changes in the protein is suggested. Within the pH range of 7 to 5.5, decreased stability of domain 1 might be associated with a decrease in the level of electrostatic attraction that occurs upon protonation of acidic residues. CLIC1 has three histidines, 12 aspartates and 21 glutamates. Inspection of the crystal structure (PDB code 1k0m) indicates that none of the histidine residues are directly involved in side chain-side chain interactions with other residues but are involved in water-mediated hydrogen bonding. At this stage it is not clear if and how protonation of these histidines might impact the conformation of CLIC1. It is interesting to note that a histidine residue (His74) is located in a segment (peptide 68−82) that displays enhanced H/D exchange when the pH is lowered from 7 to 5.5 (Figure 7A). Domain 1 has two salt bridges (Arg29−Glu81 and Lys37−Glu85), while one exists across the domain interface (Lys20−Asp225). Interestingly, these salt bridges involve residues located in the two segments (peptide 11−31 and peptide 68−82) that display significantly enhanced H/D-exchange rates at pH 5.5 (Figure 7A). Although the pK_a values of the acidic partners are unknown, it is tempting to speculate that at a low pH they may become protonated and neutral (at least partly at pH 5.5). Since Arg29 and Lys37 are buried at the domain interface, their positively charged side chains would diminish the conformational stability of the respective regions, making them more mobile, in accordance with the exchange data. Furthermore, disruption of the Arg29−Glu81 salt bridge between helices 1 and 3 could also destabilize the interdomain interaction at Met32. Once domain 1 is destabilized and primed within the acidic environment at the surface of a membrane, the presence of an acidic lipid bilayer may induce the domain to unfold, exposing the transmembrane region which is then driven to undergo conformational changes and insert into the membrane.

SUPPORTING INFORMATION AVAILABLE

Two figures as described in the text. This material is available free of charge via the Internet at http://pubs.acs.org.

REFERENCES

1. Ashley, R. H. (2003) Challenging accepted ion channel biology: p64 and the CLIC family of putative intracellular anion channel proteins. *Mol. Membr. Biol. 20*, 1–11.
2. Schlesinger, P. H., Blair, H. C., Teitelbaum, S. L., and Edwards, J. C. (1997) Characterization of the osteoclast ruffled border chloride channel and its role in bone resorption. *J. Biol. Chem. 272*, 18636–18643.
3. Ronnov-Jessen, L., Villadsen, R., Edwards, J. C., and Petersen, O. W. (2002) Differential expression of a chloride intracellular channel gene, CLIC4, in transforming growth factor-beta1-mediated conversion of fibroblasts to myofibroblasts. *Am. J. Pathol. 161*, 471–480.
4. Fernandes-Salas, E., Suh, K. S., Speransky, V. V., Bowers, W. L., Levy, J. M., and Adams, T.; et al. (2002) mtCLIC/CLIC4, an organellular chloride channel protein, is increased by DNA damage and participates in the apoptotic response to p53. *Mol. Cell. Biol. 22*, 3610–3620.
5. Suh, K. S., Mutoh, M., Gerdes, M., Crutchley, J. M., Mutoh, T., and Edwards, L. E.; et al. (2005) Antisense suppression of the chloride intracellular channel family induces apoptosis, enhances tumor necrosis factor {alpha}-induced apoptosis, and inhibits tumor growth. *Cancer Res. 65*, 562–571.
6. Berry, K. L., Bülow, H. E., Hall, D. H., and Hobert, O. A (2003) A *C. elegans* CLIC-like protein required for intracellular tube formation and maintenance. *Science 302*, 2134–2137.
7. Novarino, G., Fabrizi, C., Tonini, R., Denti, M. A., Malchiodi-Albedi, F., Lauro, G. M., Sacchetti, B., Paradisi, S., Ferroni, A., Curmi, P. M., Breit, S. N., and Mazzanti, M. (2004) Involvement of the intracellular ion channel CLIC1 in microglia-mediated beta-amyloid-induced neurotoxicity. *J. Neurosci. 24*, 5322–5330.
8. Tonini, R., Ferroni, A., Valenzuela, S. M., Warton, K., Campbell, T. J., Breit, S. N., and Mazzanti, M. (2000) Functional characterisation

of the NCC27 nuclear protein in stable transfected CHO-K1 cells. *FASEB J. 14*, 1171–1178.
9. Tulk, B. M., Schlesinger, P. H., Kapadia, S. A., and Edwards, J. C. (2000) CLIC-1 functions as a chloride channel when expressed and purified from bacteria. *J. Biol. Chem. 275*, 26986–26998.
10. Tulk, B. M., Kapadia, S., and Edwards, J. C. (2002) CLIC1 inserts from the aqueous phase into phospholipid membranes, where it functions as an anion channel. *Am. J. Physiol. 282*, C1103–C1112.
11. Harrop, S. J., De Maere, M. Z., Fairlie, W. D., Rezstsova, T., Valenzuela, S. M., Mazzanti, M., Tonini, R., Qiu, M. R., Jankova, L., Warton, K., Bauskin, A. R., Wu, W. M., Pankhurst, S., Campbell, T. J., Breit, S. N., and Curmi, P. M. G. (2001) Crystal structure of a soluble form of the intracellular chloride ion channel CLIC1 (NCC27) at 1.4 Å resolution. *J. Biol. Chem. 276*, 44993–45000.
12. Littler, D. R., Harrop, S. J., Fairlie, D., Brown, L. J., Pankhurst, G. J., Pankhurst, S., DeMaere, M. Z., Campbell, T. J., Bauskin, A. R., Tonini, R., Mazzanti, M., Breit, S. N., and Curmi, P. M. G. (2004) The intracellular chloride ion channel protein CLIC1 undergoes a redox-controlled structural transition. *J. Biol. Chem. 279*, 9298–9305.
13. Li, Y. F., Li, D. F., Zeng, Z. H., and Wang, D. C. (2006) Trimeric structure of the wild soluble chloride intracellular ion channel CLIC4 observed in crystals. *Biochem. Biophys. Res. Commun. 343*, 1272–1278.
14. Littler, D. R., Harrop, S. J., Brown, L. J., Pankhurst, G. J., Mynott, A. V., Luciani, P., Mandyam, R. A., Mazzanti, M., Tanda, S., Berryman, M. A., Breit, S. N., and Curmi, P. M. G. (2007) Comparison of vertebrate and invertebrate CLIC proteins: The crystal structures of *Caenorhabditis elegans* EXC-4 and *Drosophila melanogaster* DmCLIC. *Proteins 71*, 364–378.
15. Littler, D. R., Assaad, N. N., Harrop, S. J., Brown, L. J., Pankhurst, G. J., Luciani, P., Aguilar, M.-I., Mazzanti, M., Berryman, M. A., Breit, S. N., and Curmi, P. M. G. (2005) Crystal structure of the soluble form of the redox-regulated chloride ion channel protein CLIC4. *FEBS J. 272*, 4996–5007.
16. Mi, W., Liang, Y. H., Li, L., and Su and, X. D. (2008) The crystal structure of human chloride intracellular channel protein 2: A disulfide bond with functional implications. *Proteins 71*, 509–513.
17. Cromer, B. A., Gorman, M. A., Hansen, G., Adams, J. J., Coggan, M., Littler, D. R., Brown, L. J., Mazzanti, M., Breit, S. N., Curmi, P. M. G., Dulhunty, A. F., Board, P. G., and Parker, M. W. (2007) Structure of the Janus Protein Human CLIC2. *J. Mol. Biol. 374*, 719–731.
18. Duncan, R. R., Westwood, P. K., Boyd, A., and Ashley, R. H. (1997) Rat brain p64H1, expression of a new member of the p64 chloride channel protein family in endoplasmic reticulum. *J. Biol. Chem. 272*, 23880–23886.
19. Singh, H., and Ashley, R. H. (2006) Redox regulation of CLIC1 by cysteine residues associated with the putative channel pore. *Biophys. J. 90*, 1628–1638.
20. Berry, K. L., and Hobert, O. (2006) Mapping functional domains of chloride intracellular channel (CLIC) proteins *in vivo*. *J. Mol. Biol. 359*, 1316–1333.
21. von Heijne, G., and Blomberg, C. (1979) Trans-membrane translocation of proteins. The direct transfer model. *Eur. J. Biochem. 97*, 175–181.
22. Epand, R. M. (1998) Lipid polymorphism and protein-lipid interactions. *Biochim. Biophys. Acta 1376*, 353–368.
23. Chenal, A., Savarin, P., Nizard, P., Guillain, F., Gillet, D., and Forge, V. (2002) Membrane protein insertion regulated by bringing electrostatic and hydrophobic interactions into play. A case study with the translocation domain of diphtheria toxin. *J. Biol. Chem. 277*, 43425–43432.
24. Johnson, J. E., Xie, M., Singh, L. M., Edge, R., and Cornell, R. B. (2003) Both acidic and basic amino acids in an amphitropic enzyme, CTP:phosphocholine cytidyltransferase, dictate its selectivity for anionic membranes. *J. Biol. Chem. 278*, 514–522.
25. Yoshida, Y., Kinuta, M., Abe, T., Liang, S., Araki, K., and Cremona, O. (2004) The stimulatory action of amphiphysin on dynamin function is dependent on lipid bilayer curvature. *EMBO J. 23*, 3483–3491.
26. Chenal, A., Vernier, G., Savarin, P., Bushmarina, N. A., Gèze, A., Guillain, F., Gillet, D., and Forge, V. (2005) Conformational states and thermodynamics of α-lactalbumin bound to membranes: a case study of the effects of pH, calcium, lipid membrane curvature and charge. *J. Mol. Biol. 349*, 890–905.
27. Goodchild, S. C., Howell, M. W., Cordina, N. M., Littler, D. R., Breit, S. N., Curmi, P. M. G., and Brown, L. J. (2009) Oxidation promotes insertion of the CLIC1 chloride intracellular channel into the membrane, in press.
28. Warton, K., Tonini, R., Fairlie, W. D., Mathews, J. M., Valenzuela, S. M., Qiu, M. R., Wu, W. M., Pankhurst, S., Bauskin, A. R., Harrop, S. J., Campbell, T. J., Curmi, P. M. G., Breit, S. N., and Mazzanti, M. (2002) Recombinant CLIC1 (NCC27) assembles in lipid bilayers via a pH-dependent two-state process to form chloride ion channels with identical characteristics to those observed in Chinese hamster ovary cells expressing CLIC1. *J. Biol. Chem. 277*, 26003–26011.
29. McLaughlin, S. (1989) The electrostatic properties of membranes. *Annu. Rev. Biophys. Biophys. Chem. 18*, 113–136.
30. Menestrina, G., Forti, S., and Gambale, F. (1989) Interaction of tetanus toxin with lipid vesicles. Effects of pH, surface charge, and transmembrane potential on the kinetics of channel formation. *Biophys. J. 55*, 393–405.
31. van der Goot, F. G., González-Manãs, J. M., Lakey, J. H., and Pattus, F. (1991) A 'molten-globule' membrane-insertion intermediate of the pore-forming domain of colicin A. *Nature 354*, 408–410.
32. Parker, M. W., and Feil, S. C. (2005) Pore-forming protein toxin: from structure to function. *Prog. Biophys. Mol. Biol. 88*, 91–142.
33. London, E. (1992) Diphtheria toxin: membrane interaction and membrane translocation. *Biochim. Biophys. Acta 1113*, 25–51.
34. Lacy, D. B., and Stevens, R. C. (1998) Unraveling the structures and modes of action of bacterial toxins. *Curr. Opin. Struct. Biol. 8*, 778–784.
35. Zakharov, S. D., and Cramer, W. A. (2002) Colicin crystal structures: pathways and mechanisms for colicin insertion into membranes. *Biochim. Biophys. Acta 1565*, 333–346.
36. Black, B. E., Foltz, D. R., Chakravarthy, S., Luger, K., Woods, V. L. Jr., and Cleveland, D. W. (2004) Structural determinants for generating centromeric chromatin. *Nature 430*, 578–582.
37. Brudler, R., Gessner, C. R., Li, S., Tyndall, S., Getzoff, E. D., and Woods, V. L. Jr. (2006) PAS domain allostery and light-induced conformational changes in photoactive yellow protein upon I2 intermediate formation, probed with enhanced hydrogen/deuterium exchange mass spectrometry. *J. Mol. Biol. 363*, 148–160.
38. Burns-Hamuro, L. L., Hamuro, Y., Kim, J. S., Sigala, P., Fayos, R., Stranz, D. D., Jennings, P. A., Taylor, S. S., and Woods, V. L. Jr. (2005) Distinct interaction modes of an AKAP bound to two regulatory subunit isoforms of protein kinase A revealed by amide hydrogen/deuterium exchange. *Protein Sci. 14*, 2982–2992.
39. Del Mar, C., Greenbaum, E. A., Mayne, L., Englander, S. W., and Woods, V. L. Jr. (2005) Structure and properties of alpha-synuclein and other amyloids determined at the amino acid level. *Proc. Natl Acad. Sci. U.S.A. 102*, 15477–15482.
40. Valenzuela, S. M., Martin, D. K., Por, S. B., Robbins, J. M., Warton, K., Bootcov, M. R., Schofield, P. R., Campbell, T. J., and Breit, S. N. (1997) Molecular cloning and expression of a chloride ion channel of cell nuclei. *J. Biol. Chem. 272*, 12575–12582.
41. Bai, Y., Milne, J. S., Mayne, L., and Englander, S. W. (1993) Primary structure effects on peptide group hydrogen exchange. *Proteins: Struct., Funct., Genet. 17*, 75–86.
42. Zhang, Z., and Smith, D. L. (1993) Determination of amide hydrogen exchange by mass spectrometry: a new tool for protein structure elucidation. *Protein Sci. 2*, 522–531.
43. Fanucchi, S., Adamson, R. J., and Dirr, H. W. (2008) Formation of an unfolding intermediate state of soluble chloride intracellular channel protein CLIC1 at acidic pH. *Biochemistry 47*, 11674–11681.
44. Thompson, L. C., Walters, J., Burke, J., Parsons, J. F., Armstrong, R. N., and Dirr, H. W. (2006) Double mutation at the subunit interface of glutathione transferase rGSTM1−1 results in a stable, folded monomer. *Biochemistry 45*, 2267–2273.
45. Stenberg, G., Dragani, B., Cocco, R., Mannervik, B., and Aceto, A. (2000) A conserved "hydrophobic staple motif" plays a crucial role in the refolding of human glutathione transferase P1-1. *J. Biol. Chem. 275*, 10421–10426.
46. Manceva, S. D., Pusztai-Carey, M., and Butko, P. (2004) Effect of pH and ionic strength on the cytolytic toxin Cyt1A: a fluorescence spectroscopy study. *Biochim. Biophys. Acta 1699*, 123–130.
47. Parker, M. W., Tucker, A. D., Tsernoglou, D., and Pattus, F. (1990) Insights into membrane insertion based on studies of colicins. *Trends Biochem. Sci. 15*, 126–129.
48. Blewitt, M. G., Chung, L. A., and London, E. (1985) Effect of pH on the conformation of diphtheria toxin and its implications for membrane penetration. *Biochemistry 24*, 5458–5464.
49. Bychkova, V. E., Dujsekina, A. E., Klenin, S. I., Tiktopulo, E. I., Uversky, V. N., and Ptitsyn, O. B. (1996) Molten globule-like state of cytochrome c under conditions simulating those near the membrane surface. *Biochemistry 35*, 6058–6063.
50. Song, M., Shao, H., Mujeeb, A., James, T. L., and Miller, W. L. (2001) Molten−globule structure and membrane binding of the N-terminal

protease-resistant domain (63−193) of the steroidogenic acute regulatory protein (StAR). *Biochem. J. 356*, 151–158.
51. Nam, G. H., and Choi, K. Y. (2002) Association of human tumor necrosis factor-related apoptosis inducing ligand with membrane upon acidification. *Eur. J. Biochem. 269*, 5280–5287.
52. Thuduppathy, G. R., Terrones, O., Craig, J. W., Basañez, G., and Hill, R. B. (2006) The N-terminal domain of Bcl-XL reversibly binds membranes in a pH-dependent manner. *Biochemistry 45*, 14533–14542.
53. Lacroix, E., Viguera, A. R., and Serrano, L. (1998) Elucidating the folding problem of a-helices: local motifs, long-range electrostatics, ionic strength dependence and prediction of NMR parameters. *J. Mol. Biol. 284*, 173–191.
54. Scholtz, J. M., and Baldwin, R. L. (1992) *Annu. Rev. Biophys. Biomol. Struct. 21*, 95–118.
55. Ladner, J. E., Parsons, J. F., Rife, C. L., Gilliand, G. L., and Armstrong, R. N. (2004) Parallel evolutionary pathways for glutathione transferases: structure and mechanism of the mitochondria class kappa enzyme rGST K1-1. *Biochemistry 43*, 352–361.
56. Wang, S., Trumble, W. R., Liao, H., Wesson, C. R., Dunker, A. K., and Kang, C. (1998) Crystal structure of calsequestrin from rabbit skeletal muscle sarcoplasmic reticulum. *Nat. Struct. Biol. 5*, 476–483.